Eur. Phys. J. A **2**, 411–415 (1998)

THE EUROPEAN PHYSICAL JOURNAL A

Kinetic energy spectrum and polarization of neutrons from the reaction $^{12}C(\vec{p},\vec{n})X$ at 590 MeV

J. Arnold[1], B. van den Brandt[3], M. Daum[3,b], M. Finger[4,5], M. Finger, Jr.[5], J. Franz[1], N. Goujon-Naef[2], P. Hautle[3], R. Hess[2,a], A. Janata[5], J.A. Konter[3], H. Lacker[1], C. Lechanoine-Leluc[2], F. Lehar[6], S. Mango[3], D. Rapin[2], E. Rössle[1], R. Schirmaier[1], P.A. Schmelzbach[3], M. Schmidt[1], H. Schmitt[1], P. Sereni[1], M. Slunecka[4,5], A. Teglia[2], B. Vuaridel[2]

[1] Fakultät für Physik der Universität Freiburg, D-79104 Freiburg, Germany
[2] DPNC, Université de Genève, CH-1211 Genève, Switzerland
[3] PSI, Paul-Scherrer-Institut, CH-5232 Villigen-PSI, Switzerland
[4] MFF, Karlova Universita, CZ-18000 Praha, Czech Republic
[5] LNP, Joint Institute for Nuclear Research, RU-141980 Dubna, Russia
[6] DAPNIA/SSP, CEA-Saclay, F-91191 Gif-sur-Yvette, France

Received: 3 April 1998
Communicated by B. Povh

Abstract. The kinetic energy spectrum and the polarization of the PSI neutron beam produced in the reaction $^{12}C(\vec{p},\vec{n})X$ at 0° with 590 MeV polarized protons were investigated. A strong energy dependence of the neutron beam polarization is observed which was not expected at the time the neutron beam was built.

PACS. 29.25.Dz Neutron sources – 25.40.Ve Other reactions above meson production thresholds – 13.75.Cs Nucleon-nucleon interactions (including antinucleons, deuterons etc.)

1 Introduction

An experimental facility was built at the Paul-Scherrer-Institut (PSI) for experiments using high intensity proton or neutron beams. The beams may be either polarized or unpolarized. A detailed description of the whole facility, named NA2, is given in [1, 2].

In particular, polarized neutrons are produced in the reaction

$$C(\vec{p},\vec{n})X \qquad (1)$$

by 590 MeV polarized protons incident on a 12 cm long graphite target with a density $\rho = 1.75\,\mathrm{g/cm^3}$. The neutron beam, extracted at an angle of 0° with respect to the incoming proton beam, has a polarization of $20\,\% \leq P_\mathrm{n} \leq 50\,\%$ for kinetic energies $250\,\mathrm{MeV} \leq T_\mathrm{n} \leq 560\,\mathrm{MeV}$. The $(\vec{p},\vec{n})$ polarization transfer from longitudinally polarized protons was found to be most efficient for producing polarized neutrons at very forward angles [2].

In the present paper, we describe precise measurements of the polarization and the energy spectrum of the NA2 neutron beam. This information is essential for the analysis of all spin-dependent observables.

2 Experimental set-up

The experiment is based on free neutron-proton (np) elastic scattering. It relied on the detection of the forward recoiling proton in the angular region $23° \leq \theta_\mathrm{p} \leq 37°$ where the np analyzing power is large. The experimental set-up, shown in Fig. 1, consisted of (i) a 3.15 cm thick liquid hydrogen target (LH_2), placed 24 m downstream of the neutron production target; (ii) a magnetic spectrometer equipped with drift chambers (CH1 – CH4) for the determination of the scattering angles and the momentum of the recoil protons; (iii) a proton time-of-flight (TOF) system consisting of a 3 mm thick scintillation counter S1 behind CH1 and a hodoscope S2 made of five vertical overlapping scintillators, each 20 cm wide and 10 mm thick, placed behind CH4; (iv) an array of two times 8 horizontal scintillator bars (NB), $10\times10\,\mathrm{cm^2}$ across and 1 m long to detect the scattered neutrons; (v) an array of 5 mm thick scintillators V in front of the neutron detector which served as a veto counter to reject charged particles.

A first-level trigger required a coincidence between S1 and S2. A second-level trigger, requiring a signal in CH1 in front of S1 within 600 ns after the S1·S2 coincidence, rejected most of the np events produced in S1. The events from this second-level trigger constituted the "one-arm" data set used for the extraction of the kinetic energy spec-

[a] Deceased
[b] E-mail address: Manfred.Daum@PSI.CH

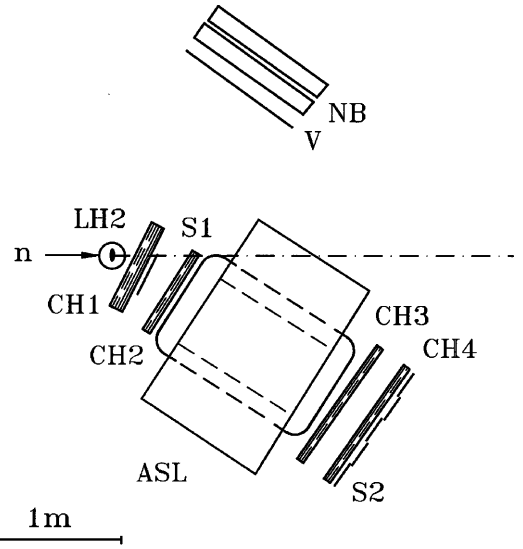

Fig. 1. Experimental set-up to measure the energy spectrum and the polarization of the neutron beam. n: neutron beam; LH_2: liquid hydrogen target; CH1 - CH4: drift chambers in the proton spectrometer; S1: start counter; ASL: spectrometer magnet; S2: stop counter hodoscope; V: veto counter array to reject charged particles; NB: scintillation counter bars for neutron detection

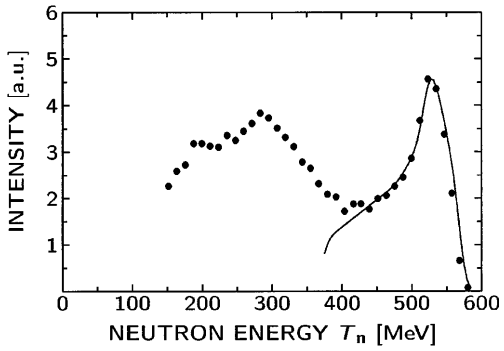

Fig. 2. Measured neutron spectrum produced in the reaction $^{12}C(\vec{p},\vec{n})X$ at 0°, as a function of the kinetic energy T_n (full dots). The smooth curve was calculated using a measured excitation spectrum of ^{12}N (cf. [5]) as described in the text

trum and the polarization of the neutron beam. The horizontal scintillator bars NB for the detection of the associated scattered neutron were not included in the trigger but allowed the selection of a "two-arm" data subset which was used for consistency checks as discussed later in the text. At a primary proton beam intensity of 9 μA, about 200 events/s were written on tape after the second-level trigger.

In the analysis, recoil protons were identified by their mass derived from the time-of-flight between S1 and S2 (short time-of-flight, TOF_s) with a TOF_s resolution of $\sim$0.9 ns (FWHM), and by their momentum vector measured in the spectrometer. The resolution for the measurement of the recoiling proton angle was 0.07° (FWHM); the momentum resolution of the spectrometer was 3 %(FWHM). The energies of the protons were corrected for energy losses (dE/dx) in the different materials along their flight paths. The kinetic energy T_n of the incident neutron was determined from the time-of-flight between the neutron production target and the LH_2 target (long time-of-flight, TOF_l). The S1 signal served as a start to a time-to-digital converter (TDC), which was stopped by the 50.63 MHz rf-signal of the PSI ring cyclotron. The measured time was corrected for the time-of-flight of the recoil protons from the hydrogen target to S1 (cf. Fig. 1) using TOF_s. A TOF_l resolution of $\sim$0.9 ns (FWHM) was obtained, corresponding to a neutron energy resolution of 21 MeV at 550 MeV and of 4 MeV at 200 MeV (FWHM). Elastic scattering events were selected by requiring the correct matching of the incident neutron energy with the angle and the momentum of the recoil proton. This was done by comparing the measured TOF_l with the calculated time-of-flight TOF_l(calc) using the measured momentum vector of the recoil proton. From the evaluation of the difference $\Delta TOF_l = TOF_l(calc) - TOF_l$, showing narrow peaks on a flat background, the remaining background fraction of the inelastic events was determined to be 6 % of the total events. In addition, this procedure removed the ambiguities in the neutron energy which arise if only TOF_l is used.

3 Neutron energy spectrum

The energy spectrum of the incoming neutrons was obtained from the distribution of the elastic events in the "one-arm" data. A correction for the energy dependence of the elastic neutron-proton cross-section was applied. The latter was calculated from a recent phase shift solution [4]. The resulting kinetic energy spectrum of the neutrons as a function of T_n is shown in Fig. 2. The peak around 530 MeV (quasi-elastic peak) is produced in the process $^{12}C(\vec{p},\vec{n})^{12}N$, where the ^{12}N recoil nucleus is left in the ground state or in an excited state. Above 450 MeV, the measured distribution of the kinetic energies can be reproduced by a smooth curve (cf. Fig. 2) calculated from the excitation spectrum of ^{12}N as measured by Wakasa *et al.* [5] with 295 MeV protons using a very thin target. In this calculation, we took into account (i) the average energy loss of the incoming protons in the 12 cm thick neutron production target, which can amount to 48 MeV; (ii) the 17.3 MeV/c^2 mass difference $M(^{12}C) - M(^{12}N)$, and (iii) the energy resolution from the TOF_l measurement. Above 450 MeV, the excellent agreement between this calculation and our measured spectrum indicates that the nuclear charge-exchange process is probably dominant in this excitation range. For neutron energies below 400 MeV, a broad continuum characterizes the region where Δ_{33} and π production are dominant in reaction (1).

4 Neutron beam polarization

4.1 Method of analysis

The neutron beam polarization was extracted from the measurement of the asymmetry in np elastic scattering with vertically polarized neutrons assuming that the np analyzing power $A_{no}(T_n, \theta)$ is known from phase shift analyses [4,6]. For the measurement, the neutron beam polarization was rotated from the longitudinal ($\hat{z}$) to the vertical orientation ($\hat{y}$). For each event, the c.m. scattering angle θ, the azimuthal angle ϕ of the scattered neutron, and the kinetic energy T_n of the incident neutron are calculated. In the analysis, we used the method of weighted sums [7] which takes into account the azimuthal ϕ distribution and requires the symmetry of the acceptance function, $\eta(\phi) = \eta(\phi + \pi)$. This was automatically achieved by flipping the proton beam polarization every second at the polarized ion source and by rotating the origin of the ϕ angles in the analysis accordingly. The estimators for the two transverse components P_y and P_x of the beam polarization are given by:

$$\begin{pmatrix} P_y \\ -P_x \end{pmatrix} = \begin{pmatrix} \sum A^2(\theta)\cos^2\phi & \sum A^2(\theta)\sin\phi\cos\phi \\ \sum A^2(\theta)\sin\phi\cos\phi & \sum A^2(\theta)\sin^2\phi \end{pmatrix}^{-1} \times \begin{pmatrix} \sum A(\theta)\cos\phi \\ \sum A(\theta)\sin\phi \end{pmatrix} \quad (2)$$

The sums are taken over all events at all angles θ and ϕ in a fixed kinetic energy bin. The relative beam intensity and the polarization were continuously recorded by the beam monitors described in [1]. No significant difference down to the level of 10^{-3} was observed in either the intensity or the position of the neutron beam for the two states of the proton beam polarization.

4.2 Background

In order to obtain the "two-arm" data subset in the off-line analysis, a signal in the neutron detector wall was required which determined the neutron scattering angle. This information together with the measured angle of the recoil proton was matched to the kinematics of the np elastic scattering. The background originating from inelastic events from hydrogen and from the materials surrounding the target (mainly carbon) was much smaller for the "two-arm" data subset than for the "one-arm" data due to the additional constraints, i.e. coplanarity and matching of the np scattering angle. However, the statistical errors of the neutron beam polarization extracted from these "two-arm" data subsets were much larger. The average beam polarization was found to be larger for the "two-arm" data subset by factors of 1.035±0.037 and 1.027±0.024 in the energy intervals 200 – 350 MeV and 350 – 575 MeV, respectively. These factors were applied to the "one-arm" polarization results in order to correct for the background contribution.

An independent method of estimating the background correction can be derived as follows: The quasi-elastic np analyzing power of carbon is ∼0.5 – 0.7 of that for the free scattering [8]. By taking into account the 6 % background fraction in the present experiment for incident kinetic energies above 200 MeV, one obtains a polarization correction factor of 1.02 – 1.03, in agreement with the applied background corrections described above. The final errors of the polarization were obtained by adding the errors from the background correction and the statistical errors quadratically.

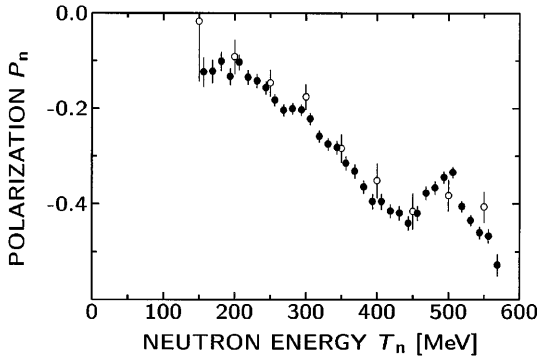

Fig. 3. Longitudinal polarization of the neutron beam P_n from the reaction $^{12}C(\vec{p},\vec{n})X$ at 0° as a function of the neutron kinetic energy T_n. Full dots: this experiment; open circles: our data from [1], measured with a different experimental set-up

4.3 Results

The measured neutron beam polarization P_n as a function of the kinetic energy T_n is shown in Fig. 3. The numerical values of the longitudinal polarization of the neutron beam as produced in the graphite target are given in Table 1

Table 1. Longitudinal neutron polarization from the reaction $^{12}C(\vec{p},\vec{n})X$ at 0° with 0.76 longitudinally polarized protons at a kinetic energy of 590 MeV; ΔP_n is the total error as discussed in the text

T_n [MeV]	P_n	ΔP_n	T_n [MeV]	P_n	ΔP_n
156	−0.124	±0.031	369	−0.332	±0.015
169	−0.123	±0.025	381	−0.365	±0.014
181	−0.101	±0.020	394	−0.395	±0.015
194	−0.133	±0.018	406	−0.396	±0.017
206	−0.104	±0.016	419	−0.415	±0.014
219	−0.135	±0.015	431	−0.419	±0.015
231	−0.143	±0.014	444	−0.441	±0.015
244	−0.157	±0.014	456	−0.420	±0.015
256	−0.183	±0.013	469	−0.378	±0.014
269	−0.204	±0.013	481	−0.366	±0.014
281	−0.201	±0.012	494	−0.345	±0.013
294	−0.204	±0.012	506	−0.334	±0.012
306	−0.222	±0.012	519	−0.406	±0.011
319	−0.259	±0.013	531	−0.435	±0.012
331	−0.275	±0.013	544	−0.461	±0.013
344	−0.282	±0.014	556	−0.467	±0.015
356	−0.315	±0.014	569	−0.528	±0.023

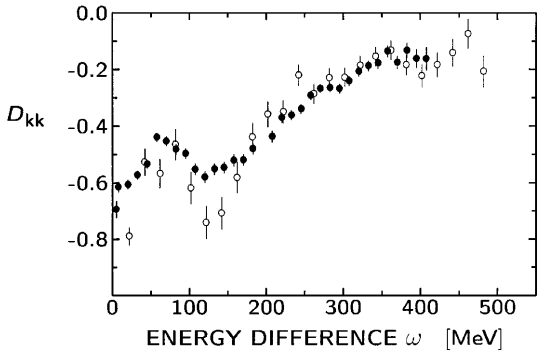

Fig. 4. Polarization transfer parameter $D_{kk}(0°)$ for the reaction $^{12}C(\vec{p},\vec{n})X$ as a function of the proton energy loss $\omega = T_p(\text{in}) - T_n(\text{out})$. Full dots: this experiment; open circles: data from Ref. [9]. For our data, an incident proton energy of 565 MeV was used to calculate ω, taking into account an average energy loss of the protons of 24 MeV corresponding to one half of the target thickness

along with the total errors ΔP_n as discussed above. The original longitudinal polarization of the neutron beam is obtained from the measured vertical polarization P_y (cf. (2)) by

$$P_n = \frac{P_y}{\sin\alpha}\,, \tag{3}$$

where the spin rotation angle α in the dipole magnet downstream of the neutron production target depends on the neutron energy. These results agree well with our earlier measurement [1] (open circles in Fig. 3), for which a different experimental set-up was used. In the present data however, a significant structure in the energy dependence of the neutron beam polarization which could not be resolved in our previous data [1], was found around 500 MeV.

The presence of the quasi-elastic peak in the energy distribution of the incident neutrons might produce an energy-dependent structure in the asymmetry measurement if the measured neutron energy depends on the primary beam polarization or on the counting rate of the detectors. In order to exclude an instrumental origin of the measured asymmetry, we used photons from π^0 decay in the neutron production target and found that our time-of-flight measurement did not depend either on the beam intensity or on the beam polarization. A further test was made using the "two-arm" data subset. For these events the incoming neutron energy can be determined independently of the TOF_l measurement using only the kinematic data from the analysis of the recoil protons in the spectrometer. In all cases, no influence on the measured beam polarization was found.

The parameter $D_{kk}(0°)$ for the longitudinal polarization transfer in reaction (1) is obtained from the value of P_n by normalization to the proton beam polarization P_p

$$D_{kk} = \frac{P_n}{P_p} \tag{4}$$

with $P_p = 0.76$ in this experiment [1]. The resulting values for D_{kk} are shown in Fig. 4 as a function of the energy loss ω defined as the difference between the kinetic energies of the incident proton and the outgoing neutron. Here, the energy dependent structure appears around $\omega = 60$ MeV.

Recently, data on the polarization transfer $^{12}C(\vec{p},\vec{n})$ at the same neutron extraction angle of 0° as in our experiment but with 795 MeV protons were published [9]. The values of D_{kk} in this experiment are also shown in Fig. 4. A structure similar to the one described above is observed, even though the experiment of [9] and ours were performed at different energies of the incident protons and with different target thicknesses for the neutron production. For energy losses in reaction (1) greater than 180 MeV, the reaction mechanism is dominated by Δ_{33} production. In this energy-loss region, our results are in excellent agreement with those of [9].

In 1993, the polarization transfer parameter D_{kk} at a neutron extraction angle of 0° has been measured at LAMPF [10] with a proton beam of 318 and 494 MeV. There, the final state of the recoil nucleus (ground state $^{12}N_{g.s.}$, or excited state) could be identified due to the excellent energy resolution achieved with long flight paths and a thin carbon target. When in that experiment the final state reached in reaction (1) was the nitrogen ground state $^{12}N_{g.s.}$, the value of $D_{kk}(0°)$ was found to be significantly more negative than those for the free np charge exchange (CEX), e.g. at 494 MeV, $D_{kk}(^{12}N_{g.s.}) \approx -0.7$, whereas $D_{kk}(\text{CEX}) \approx -0.5$. A similar difference was observed at 318 MeV [10]. On the other hand, if the recoil nucleus is left in an excited state with large spin, then a smaller polarization transfer is expected [11], i.e. D_{kk} is less negative. This latter effect in combination with the according energy losses (0 – 48 MeV) of the protons before reaction (1) in the 12 cm long neutron production target may explain the smooth decrease of the polarization of the outgoing neutrons between 500 and 560 MeV (see Fig. 3).

5 Conclusion

In summary, the kinetic energy spectrum and the polarization transfer coefficient $D_{kk}(0°)$ were measured for the reaction $^{12}C(\vec{p},\vec{n})X$ at 590 MeV. A strong energy-dependent structure in the neutron beam polarization around 500 MeV was observed. This effect was unexpected when the NA2 beam was designed but was recently also observed with 795 MeV polarized protons at LAMPF [9]. A decrease in the magnitude of the polarization between 560 and 500 MeV can be qualitatively understood but additional work is clearly needed to make consistent explanations of the $(\vec{p},\vec{n})$ results.

We are grateful to F. Osterfeld[a] for helpful discussions on the polarization transfer mechanism in nuclei. This experiment was supported by the German Bundesminister für Bildung, Wissenschaft und Forschung (BMBF) and the Fonds National Suisse de la Recherche Scientifique.

[a] deceased

References

1. J. Arnold *et al.*, Nucl. Instr. and Meth. in Phys. Res. A**386** (1997) 211
2. Ch. Brönnimann *et al.*, Nucl. Instr. and Meth. in Phys. Res A**343** (1994) 331
3. R. Binz *et al.*, Phys. Lett. B**231** (1989) 323
4. R.A. Arndt *et al.*, Phys. Rev. D**45** (1992) 3995, solution SM96
5. T. Wakasa *et al.*, Phys. Rev. C**51** (1995) R2871, and private communication
6. J. Bystricky *et al.*, J. Physique (France) **48** (1987) 199
7. D. Besset *et al.*, Nucl. Instr. and Meth. **166** (1979) 515
8. R. Todenhagen, Diplomarbeit, Freiburg 1988 (unpublished)
9. D. L. Prout *et al.*, Phys. Rev. Lett. **76** (1996) 4488
10. D. J. Mercer *et al.*, Phys. Rev. Lett. **71** (1993) 684
11. F. Osterfeld, Rev. of Mod. Phys. **64** (1992) 491